Refereed Proceedings

The 12th International Conference on Fluidization - New Horizons in Fluidization Engineering

Engineering Conferences International *Year* 2007

Fluid Mechanical Phenomena of Liquid-Solid Fluidization in the Centrifugal Field

Jan Margraf * Joachim Werther†

*Hamburg University of Technology, margraf@tu-harburg.de

†Hamburg University of Technology, werther@tu-harburg.de

FLUID MECHANICAL PHENOMENA OF LIQUID-SOLID FLUIDIZATION IN THE CENTRIFUGAL FIELD

Jan Margraf and Joachim Werther
Institute of Solids Process Engineering and Particle Technology
Hamburg University of Technology
Hamburg, Germany

ABSTRACT

The flow pattern in a rotating liquid-solid fluidized bed with particles in the micron range was investigated in the bed and in the freeboard. Simulations of the liquid flow in absence of particles with the CFD-Software CFX 5.7 showed a strong influence of the Coriolis force, which results in high tangential velocities. Experiments in a 1 m diameter rotor confirmed the results of the simulation. The fluidized bed is also moving in the tangential direction. The bed expansion is described by a Richardson-Zaki type correlation.

INTRODUCTION

Fluidized beds are mostly used for gas-solid systems, applications of liquid-solid systems are relatively scarce. One application is the classification of polydisperse particles in the elutriator. The separation effect is caused by an upstream in the classification chamber, which takes the fines to an overflow weir at the top, while the coarse particles accumulate in the fluidized bed due to gravity. The elutriator allows a sharp separation and is therefore widely used in the mineral processing industries for the classification of suspensions (1). The classification is practically limited to cut sizes of several hundreds of microns due to the low terminal velocities of small particles. To enable a classification of micro-particles it is necessary to enhance the settling velocities by transferring the classification into the centrifugal field (2-5). For this reason a prototype of a “Centrifugal Fluidized Bed Upstream Classifier” was developed (6-8) (figure 1). Tests with this apparatus showed satisfactory separation efficiency curves at cut sizes of a few microns. One problem was the existence of the fines in the fluidized bed (i.e. in the coarse fraction), which could not be elutriated. The main differences to the gravity elutriation are the effect of the radially varying centrifugal acceleration and the influence of the Coriolis force. To improve the performance of the classifier it is important to gain more knowledge about these influences and to study the behavior of the fluidized bed and the freeboard. For this purpose simulations of the pure liquid flow (i.e. conditions in the solids-free chamber or in the freeboard of the fluidized bed,

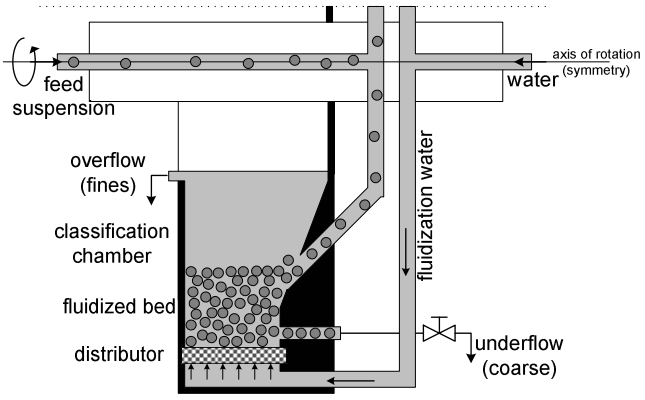

Figure 1: Sketch of the apparatus

The 12th International Conference on Fluidization - New Horizons in Fluidization Engineering, Art. 37 [2007]

respectively) with the CFD software CFX were performed in the present work and experiments were carried out to verify the findings of the simulation and to describe the behavior of the fluidized bed.

THE CFD MODEL

As the conditions in the centrifugal field are quite unusual compared to normal gravity, CFD simulations were carried out to investigate the behavior of a flowing medium in a centrifugal environment. In the simulation part only pure water (without particles) at 10℃ was considered. The whole simulation was carried out under stationary conditions. For the fluid (water) a density ρ_w=999 kg/m^3 and a viscosity η=0.0013 kg/m·s was used.

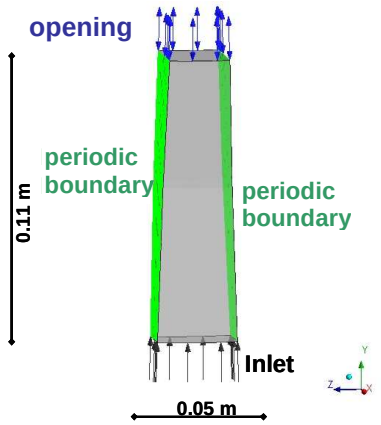

Figure 2: Model of the classification chamber

Geometry

The classification chamber can be considered as a body of revolution around the x-axis, i.e. the chamber is symmetric concerning the x-axis. The symmetry permits to consider a small section (4 degrees) of the classification chamber. The consideration of a small section enables a high mesh refinement, so that in the wall region, where the highest velocity gradients occur a cell width of 0.1 mm can be achieved. The whole model of the chamber consists of 236,811 hexahedron cells and has a height of 110 mm and a width of 20-25 mm.

Boundary Conditions

In the real chamber a porous distributor plate is used for water inlet. To simplify the calculation and to increase the robustness of the solver the porous distributor is not considered. Instead an inlet is modeled at the bottom (figure 2) with a given velocity in radial direction only.

On top of the chamber the fluid leaves the fluid domain. This boundary is modeled as an opening with a relative pressure of 0 Pa. An opening allows in and outflow through the boundary. Although all the fluid leaves the chamber at that plane an opening was recommended by CFX for stability reasons (9).

Periodic boundaries on the cut surfaces let a fluid element, which leaves the chamber on one side, reenter on the other side.

The side walls of the classification chamber are modeled as no slip boundary conditions.

The fluid domain

The equations system solved by CFX are the “Reynolds Averaged Navier Stokes” (RANS) equations for a single fluid. Averaging the velocity, which consists of a stationary and a fluctuating part, results in a turbulence term in the momentum balance. The turbulence term is solved by the k-Ω model, which describes the turbulent kinetic energy k and the turbulent frequency Ω. The k-Ω model was chosen as it shows a high robustness and accuracy (9). The rotation is modeled by adding a Coriolis and Centrifugal term to the momentum equations.

EXPERIMENTAL

Due to high angular velocities of the classifier the influence of the Coriolis force has to be examined. Schmidt (6) concluded that the Coriolis force acting on particles can

be neglected. However, the Coriolis force acting on the flow cannot be ignored as the present calculations have shown. The Coriolis force induces a velocity into the tangential direction. Experiments were performed to describe the influence of the Coriolis force on the fluidized bed and on the liquid flow in the freeboard. Further experiments were carried out to study the expansion of the bed.

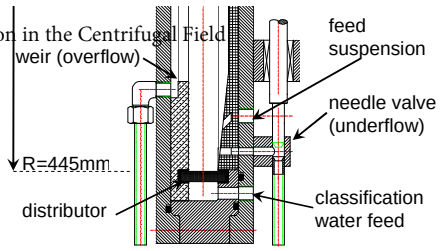

Figure 3: Classification chamber

The setup of the apparatus

The classification water and the suspension are fed into the apparatus by a rotary feedthrough from opposite sides (figure 1). Particles are introduced through suspension feed pipes into the classification chamber (figure 3) where they get in contact with the upstream, which is introduced to the chamber through a porous distributor plate. The fines are carried to an overflow weir, while the coarse settle in the fluidized bed due to centrifugal acceleration. A coarse removal is installed close above the distributor and is controlled by an elbow lever mechanism. The cut size, i.e. the condition where the drag equals the centrifugal force is one of the most important aspects concerning classification. Applying a force balance the cut size can be calculated by (6,7):

$$d_t = \sqrt{\frac{18 \cdot \eta}{(\rho_s - \rho_L) \cdot \omega^2 \cdot r} \cdot \frac{\dot{V}}{2 \cdot \pi \cdot r \cdot B}} \qquad (1)$$

As a constant cut size is desired throughout the whole classification chamber, the product r^2*B should be constant, i.e. B~r^{-2}. Due to difficulties in manufacturing this parabolic profile a linear one was used, which is very close to the ideal profile. The classification chamber is equipped with two vision panels, which enables the observation the fluidized bed and the freeboard. The observation of the fluidized bed was performed by a stroboscope and by a high-speed video camera (KODAK EKTAPRO) (figure 4).

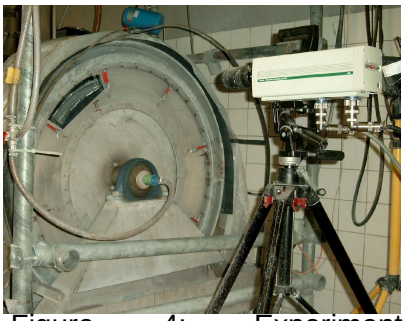

Figure 4: Experimental observation of the fluidized bed by a high speed camera

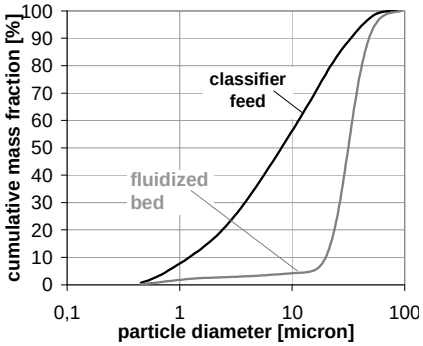

Figure 5: PSD of limestone feed and fluidized bed particles

The design of the distributor

For the fluidization of the particles a porous distributor plate made from polyethylene (CELLPOR – TYPE 152, Porex Technologies GmbH, Germany) with 8 mm thickness and a porosity of 0.46 was used. The distributor has a linear pressure drop characteristics in the range between 0 and 0.02 m/s. The pressure drop at 0.02 m/s is 0.42 bar.

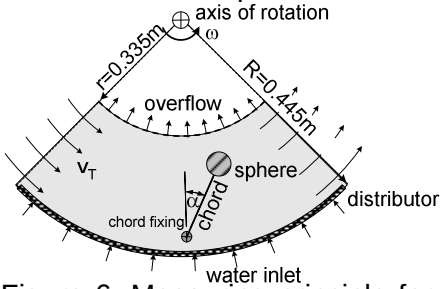

Figure 6: Measuring principle for the tangential velocity

The 12th International Conference on Fluidization - New Horizons in Fluidization Engineering, Art. 37 [2007]

Properties of the experimental materials

The materials used in the experiments were water as fluidizing medium and limestone (Saxolith 10HE, Geomin, Saxony/Germany) with a density of 2620 kg/m^3. The fluidized bed was built up in such a way that the water filled classifier was rotated at 300 rpm with 1m^3/h classification water. After the rotor has reached the desired speed the suspension feed valve was opened and 0.2 m^3/h suspension flow (solids volume content 2%) was introduced. The accumulation of solids in the fluidized bed was visually observed and the suspension feed was stopped when the desired bed height was reached. The particle size distributions of limestone in the fluid and in the fluidized bed are shown in figure 5.

Determination of the tangential velocity in the particle free zone

The determination of the tangential velocity was conducted by introducing a tracer sphere into the classification chamber and measuring its deflection angle during operation (figure 6). The sphere (diameter d_{ts} = 9.9 mm) was attached to a fixing 10 mm above the distributor by a 0.1 mm thick chord. The length of the chord was varied to be able to measure the fluid's tangential velocity at different locations in the chamber. The sphere material was plastics with a density ρ_{ts}=0.92 kg/m^3, so that it was buoying in the direction to the overflow weir. For the determination of the deflection angle, photographs were taken with the high speed video camera and graphically analyzed. To calculate the tangential velocity v_T from the deflection angle α, it is necessary to apply a force balance at the sphere in radial and tangential directions (figure 7):

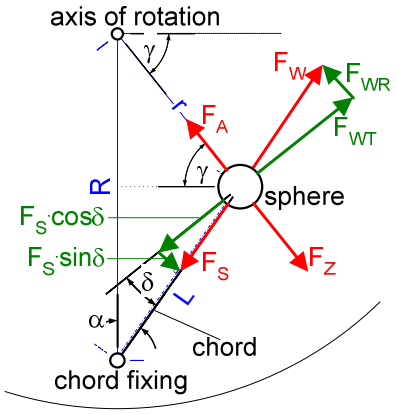

Figure 7: Force balance at the floating tracer sphere

$F_A + F_{WR} = F_Z + F_S * \sin\delta$ (2); $F_{WT} = F_S * \cos\delta$. (3);

where F_A is buoyancy force, F_Z the centrifugal force, F_{WT} the tangential drag, F_{WR} the radial drag and F_S the force on the chord.

$$F_A = V_{ts} \cdot \rho_L \cdot r \cdot \omega^2 \quad (4)$$

$$F_Z = m_{ts} \cdot r \cdot \omega^2 \quad (5)$$

$$F_{WR} = 0.17 \cdot d_{ts}^2 \cdot \rho_L \cdot \left(\frac{\dot{V}}{A_d}\right)^2 \quad (6)$$

$$F_{WT} = 0.17 \cdot d_{ts}^2 \cdot \rho_L \cdot v_T^2 \quad (7)$$

The equations (6) and (7) are valid for a fully turbulent flow at Re_{ts} > 2000. The experimental results showed that this condition was always fulfilled.

The angle δ can be calculated from the deflection angle α and the angle γ:

$\delta = \gamma - \alpha$.(8); $\gamma = \arctan[(R - L\cdot\cos\alpha)/(L\cdot\sin\alpha)]$ (9);

$r = (R^2 + L^2 - 2\cdot R\cdot L\cdot\cos\alpha)^{0,5}$ (10)

Combining the equations (2) and (3) results in

$$F_{WT} = \frac{F_A + F_{WR} - F_Z}{\tan\delta} \quad (11)$$

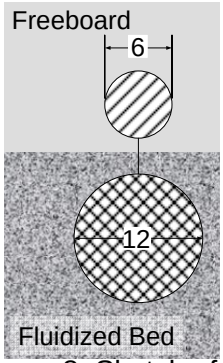

Figure 8: Sketch of tracer and indicator sphere

which leads to $$v_T = \sqrt{5.88 \cdot \frac{F_A + F_{WR} - F_Z}{d_{ts}^2 \cdot \rho_L \cdot \tan\delta}} \quad (12)$$

Determination of the tangential velocity of the fluidized bed

As the viscosity of the bed is unknown, it is not possible to determine the tangential movement of the fluidized bed by the deflection of a sphere. Since the chamber is circular, it is possible to integrate a submersed tracer body into the fluidized bed and to record its time of circulation. On top of the submersed tracer body a visible indicator is arranged for recording the location of the tracer body in the adjacent freeboard. The indicator has to be very tiny compared to the tracer, so that the influence of the liquid flow in the freeboard on the tracer is small. A sphere with a diameter d_{ts}=12mm was chosen as tracer body and a small sphere (d_i=6mm) was chosen as indicator (figure 8). The weight of the tracer was adjusted by adding some iron to achieve the desired weight, such that the tracer is completely submersed and the indicator floats above the surface of the bed. With the help of a stroboscope the vision panel of the rotating apparatus can be “frozen”, which enables to follow the movement of the indicator. With the time of circulation the tangential velocity of the bed can be determined.

Determination of the expansion behavior of the bed

Besides tangential movement of the bed and the freeboard it is also import to gain knowledge about the expansion behavior, i.e. porosity depending on rotation speed and water throughput. The porosity ε can be calculated if bed mass m_{bed}, solids density ρ_s and bed volume V_{bed} are known. The bed mass m_{bed} can be determined by recording all of the incoming and outgoing currents and concentrations during the build-up of the bed. By taking pictures of the bed through the vision panel (figure 15) it is possible to determine the bed height H_{bed} and with it the bed volume V_{bed}. The porosity can be calculated by:

$$\varepsilon = \frac{V_{bed} - M_{bed} / \rho_s}{V_{bed}} \quad (13)$$

RESULTS AND DISCUSSION

The velocity profile in the particle-free flow

The simulation of the flow in the water-filled and solids-free classification chamber is shown in figure 9. Although the injection of the flow into the classification chamber at the distributor is only radially directed, the flow pattern is mainly oriented in the tangential direction. It can be seen from the simulation result that the tangential velocity component is two orders of magnitude higher than the radial one. This can be explained by the Coriolis force, which acts in the tangential direction and reaches high values at high angular speed rates. The experimental proof of the effect of the Coriolis force is shown in figure 10: The tracer sphere is significantly deflected from the radial direction.

Additional simulations were performed at different angular speeds and radial velocities. To verify the results, an experimental determination of the tangential velocities was performed by measuring the deflection of a sphere as described above. The results of the simulations and the experimental findings can be found in figure 11. It can be seen that the experimental results match quite well the data from

The 12th International Conference on Fluidization - New Horizons in Fluidization Engineering, Art. 37 [2007]

the simulation for distributor throughputs of $\dot{V}$=1.0 m³/h and $\dot{V}$=1.3 m³/h (equals 5.0 mm/s and 6.5 mm/s superficial upstream velocity).

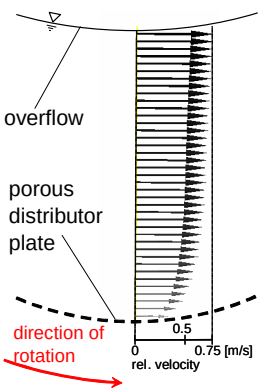

Figure 9: Simulation of pure water flow:
(angular speed ω=300 rpm, radial velocity v_R at
- distributor: 0.0050 m/s
- overflow: 0.0040 m/s)

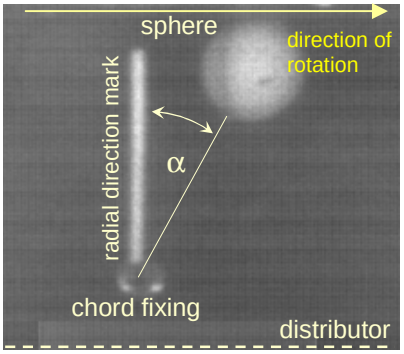

Figure 10: Photograph of the deflected sphere at 400 rpm

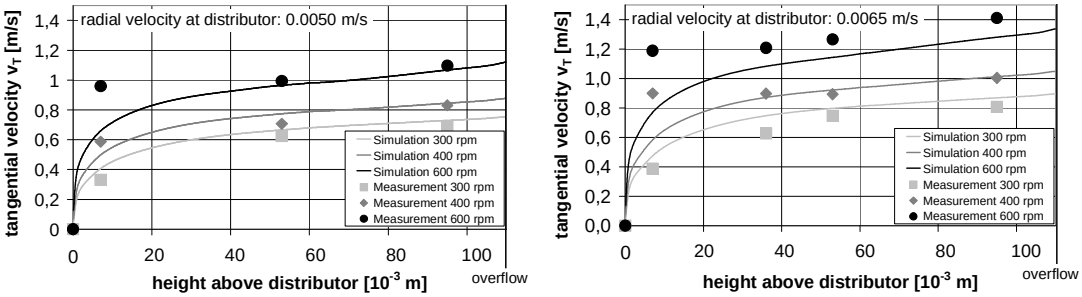

Figure 11: Comparison of simulation and measurement

The tangential velocity in the freeboard of the fluidized bed

Now the question arises, how the freeboard behaves if a fluidized bed exists below the measuring point. Therefore the deflection of the 9.9 mm diameter tracer sphere was measured at a fixed radial position 37.5 mm above the distributor at ω=300 rpm and $\dot{V}$=1 m³/h (figure 12). In this experiment the bed height was stepwise increased from 0 m to 0.031 m, i.e. 1.5 mm below the bottom line of the sphere. From the results (figure 13) it can be seen, that the tangential velocity is approximately constant with increasing bed height. Only when the surface of the bed is approaching the bottom line of the sphere a slight drop of the tangential velocity can be seen which is caused by the much slower moving fluidized bed. At distances from the bed surface exceeding 5 mm the bed has no influence on the tangential velocity, so that the values from the simulation of the pure liquid flow are valid.

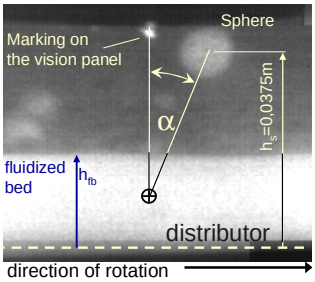

Figure 12: Photograph of the sphere above the bed

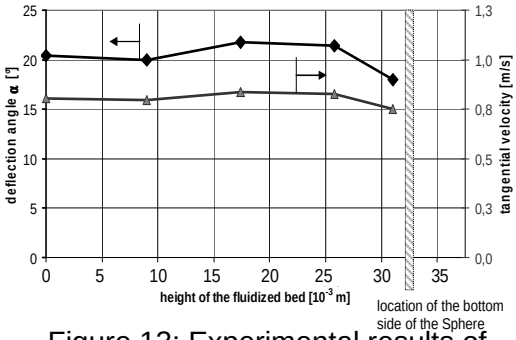

Figure 13: Experimental results of the tangential velocities in the freeboard 0.375m above the distributor at different bed heights

The tangential velocity of the bed

Now that the velocity profile in the freeboard is known it is also important to be able to describe the behavior of the bed itself. For that reason experiments were carried out with the tracer body coupled with the indicator sphere in the fluidized bed. Figure 14 shows the measured tangential velocities near the bed surface. We see that the velocities vary between 20 and 80 mm/s which is much higher than the radial velocity at the distributor which varies between 2 and 3 mm/s. On the other hand the bed velocities are much lower than the tangential liquid velocities in the freeboard (cf. figures 11,13). The tendencies are plausible. An increase of the radial velocity causes the bed to expand. The resulting higher voidage decreases the apparent bed viscosity which leads to a higher tangential velocity. The same reasoning is valid for an increase of the rotational speed which leads to a higher compaction of the bed and therefore to a lower tangential velocity.

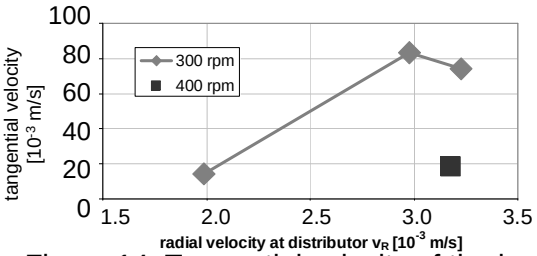

Figure 14: Tangential velocity of the bed

The expansion behavior of the bed

Experiments on the bed expansion behavior were carried out by varying the angular speed and fluidization velocity. Figure 15 shows the measurement of the height H_{fb} of the fluidized bed in the classification chamber. Figure 16 presents the results. The minimum fluidization porosity for limestone particles used here is about 0.54. All measurements in figure 16 can be approximated by a Richardson-Zaki type relationship,

$$v_R/u_t = \varepsilon^n \qquad (14)$$

with n=6.26. The numerical value of the exponent is significantly higher than the one obtained by Richardson and Zaki in their investigation of liquid fluidized beds operated under gravitational acceleration (n=4.65, (10)). It was found that the high exponent n is achieved due to the properties of the limestone. Further experiments show that other materials (quartz and glass beads) have n-values very much closer to 4.65 (n_{quartz}= 4.72 ; n_{glass} = 4.92).

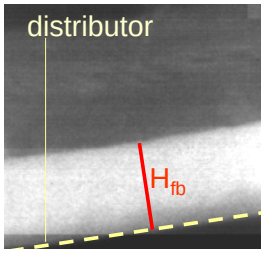

Figure 15: determination of the bed height

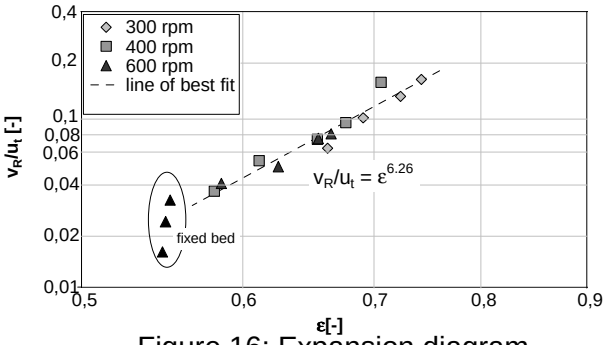

Figure 16: Expansion diagram

SUMMARY AND CONCLUSIONS

In the present paper the fluid dynamics of liquid-solid fluidized beds were investigated in the centrifugal field. First tests in the solids-free chamber revealed an intense tangential flow in the direction of rotation, which is caused by the Coriolis

The 12th International Conference on Fluidization - New Horizons in Fluidization Engineering, Art. 37 [2007]

force, resulting from the radial upstream of the liquid. Numerical simulations of the fluid flow field are confirmed by measurements in a pilot-scale apparatus. The tangential velocity is significantly higher than the radial fluid velocity. When the chamber is filled with particles a liquid fluidized bed is set up. In its freeboard the intense tangential flow is detected again. The fluidized bed itself is also moving in the tangential direction, however, with a lower velocity than the freeboard. The bed expansion can be described by a Richardson-Zaki type power law. The exponent n has a value of 6.3 for the presently investigated fine limestone particles with a mean particle size diameter of 32 μm.

NOTATION

Symbol

A_d	area of distributor [m^2]
B	width of classification chamber [m]
d_t	cut size diameter [m]
F	force [N]
n	parameter in equation (14) [-]
H_{fb}	fluidized bed height [m]
r,R	radius, radius distributor [m]
u_t	terminal velocity [m/s]
V_{ts},m_{ts},d_{ts}	volume, mass, diameter of tracer sphere [m^3],[kg],[m]
$\dot{V}$	volumetric flow [m^3/s]
v_T,v_R	fluid velocity (tangential and radial) [m/s]
V_{Bed},M_{Bed}	fluidized bed volume [m^3],mass [kg]

Greek Symbols

α	deflection angle [°]
ε	porosity [-]
η	fluid viscosity [kg/m*s]
ρ_s, ρ_w	density solid, fluid [kg/m^3]
ω	angular speed rate [rad/s]

REFERENCES

(1) Zimmels, Y.: “Elutriation” In: Ullmann’s Encyclopedia of Industrial Chemistry (B. Elvers, M.Ravenscroft, J.F.Rounsaville, G. Schulz, eds.),B2, VCH, Weinheim (1988), pp.16-1 ff.

(2) Bickert G., Stahl W., Bartsch R. and Mueller F.: “Grinding circuit for fine particles in liquid suspensions with a new counter-flow centrifugal classifier“, Int.J.Mineral Processing, 44-45, (1996), pp.733-741

(3) Colon F., van Heuven J. and van der Laan H.: ”Centrifugal elutrition of particles in liquid suspension“, Particle Size Analysis, The Society for Analytical Chemistry (J. Groves, P. Wyatt-Sargent, eds.), Bradford (1970), pp.42-52

(4) Timmermann D.: “Kontinuierliche Nassklassierung in einer Aufstromzentrifuge im Feinstkornbereich“, Dissertation, Technische Universitaet Clausthal (1998)

(5) Priesemann C.: “Nassklassierung einer Aufstromzentrifuge“, Dissertation, Technische Universität Clausthal (1994)

(6) Schmidt J.: “Wirbelschichtklassierung von Feinstkornsuspensionen im Zentrifugalfeld“, Dissertation, Technische Universität Hamburg-Harburg (2004)

(7) Schmidt J. and Werther J.: “Separation Efficiency of a Centrifugal Fluidized Bed Classifier in the Micron Range”, J. Chinese Inst. of Chem. Eng., 36 (2005), pp. 49-60

(8) Schmidt J. and Werther J.: “Simulation and Optimization of a Centrifugal Fluidized Bed Classifier in the Micron Range” Chem. Eng. Proc. 45 (2006),6, pp. 488-499

(9) Manual CFX 5.7 (2004)

(10) Richardson J.F. and Zaki W.N.: ”Sedimentation and Fluidization I“, Trans. Inst. Chem. Eng. (1954), pp.35-52